ON-ORBIT CALIBRATION OF LUNAR EXPLORATION NEUTRON DETECTORS ON BOARD LUNAR RECONNAISSANCE ORBITER AND CHARATERIZATION OF GCR PARTICLE, SECONDARY PARTICLE AND LUNAR NEUTRON COMPONENTS. J.J. Su[1](jjsu@umd.edu), R. Sagdeev[1], W.V. Boynton[2], G. Chin[3], T. Livengood[1], , T.P. McClanahan[3] A. Parsons[3], R.D. Starr[4], D. Hamara[2], K. Harshman[2], [1]Dept. of Physics, Univ. of Maryland, College Park, MD 20742 USA, [2]Lunar and Planet. Lab., Univ. Ariz., Tucson AZ 85721 USA, [3] NASA Goddard Space Flight Center, Greenbelt, MD 20771 USA, [4]The Catholic Univ. of America, Wash. D.C. 20064 USA.

Introduction: In this study, we characterize the contribution of the galactic cosmic rays (GCR), lunar neutrons, and secondary particles components to the Lunar Exploration Neutron Detector's (LEND) Collimated Sensor for Epithermal Neutrons (CSETN) and Sensor for Epithermal Neutrons (SETN) observational data to calibrate the CSETN and SETN detectors. This new calibration algorithm enables us to predict LEND's observations at any given time.

In addition to mapping the spatial distribution of hydrogen over the Moon and sensing water deposits in the permanently shaded regions at the lunar poles, the LEND is tasked with determining the neutron contribution to the total radiation dose at an altitude of 50 km above the Moon [1]. LEND's CSETN is a system with a ~10 km diameter (FWHM) field-of-view coverage of the lunar surface at a 50 km orbital altitude [2]. The CSETN spatial resolution and count rate were challenged by [3] based on the LEND team's assessment of uncollimated background contributions. In this study we provide a new CSETN and SETN calibration algorithm by cross comparing the results of Monte Carlo simulations, ground calibration data taken in Dubna [4], and cruise and on-orbit observations. Our objective in this study is to review and present the results of our new calibration methods. In this study we analyse both the omnidirectional SETN and the collimated CSETN observations, by which we can produce a multiple spatial resolution neutron maps of the Moon's south pole [5] and north pole [6] as an integratal part of achieving the LEND mission objectives.

The SETN and CSETN detectors are helium-3 (^{3}He) proportional counters that are operated in the proportional mode where the individual pulses of neutron capture events are registered. The total detected signals of SETN and CSETN can be decomposed into 1) lunar neutrons, 2) GCR protons and alpha particles, and 3) secondary particles induced by lunar neutrons interacting with the LRO spacecraft or the LEND assembly. The solar modulation potential, the LRO spacecraft altitude and the individual detector efficiencies are additional factors that will change the count rates. A change in the solar modulation potential causes changes in both the GCR flux and energy distribution and results in a change of the lunar neutron leakage flux. We used the Oulu Neutron Monitor data and the Heliospheric modulation of cosmic rays model [7] to adjust the LEND observations to the same solar modulation potential of its commissioning phase ~ 260 MV.

The proton or triton created from the ^{3}He(n,p)^{3}H reaction ionizes and excites the atoms along its path until its energy is exhausted. The GCR protons and alpha particles of energies in the range of few hundreds of MeV can be detected by ^{3}He detectors since they have a pulse signature similar to ^{3}He neutron capture. CSETN detectors are surrounded by neutron-absorbing materials to absorb thermal and epithermal neutrons approaching the detectors from large nadir angles. The collimator moderates GCR particles to a lower energy range when they penatrate the collimator wall. As a result ,some of these particles are registered as counts in the ^{3}He detectors.

We investigate the LEND performance as well as lunar neutron spallation production and transport within the lunar regolith using the Geant4[8] Monte Carlo (MC) neutron transport code. The neutron production and leakage lunar neutron spectra produced by our calculations are in good agreement with McKinney's results[9]. A complete LEND model was built to simulate the ground calibration test results obtained by the LEND team at JINR in Dubna, Russia. Our studies show that the detection efficiency of SETN's ^{3}He sensor is the same as that of CSETN ^{3}He sensors. A 25% effiencncy difference between CSETN and SETN ^{3}He sensors described in [10] originated because the neutron source had a solid angle and was not a point source. Monte Carlo simulations have shown that putting the neutron source 1.5 m from a LEND detector with zero degree incident angle will yield a count rate ratio CSETN/SETN ~ 1.25. Once the neutron source is put farther away from the detector, for example 15 m, SETN has the same count rate as the CSETN measurement. The observations from the cruise phase and insertion period also suggest that the ^{3He} sensors for SETN and CSETN have the same detection efficiency.

The GCR background contribution to the LEND data is proportional to the detectors' solid angle to the open sky, so altitude variations greatly influence background signals. The LRO spacecraft efficiently blocks part of the sky to the LEND detectors and prevents part of GCR particles from contributing to the background.

Our studies show that the open sky solid angle is about 2π for SETN and 3π for CSETN instead of 4π for free space.

Results: Figure 1 illustrates the observational background contribution from neutrons penetrating through the walls of the CSETN collimators. Figure 2 shows that about 40% of the total neutrons detected by CSETN are true "collimated" neutrons, namely where their incident angles are within 15^{o} of the instrument's bosresight. This figure shows that some of the detected neutrons approaching the LEND/LRO are at a small nadir angle. Quantifying the "collimated" and "uncollimated" neutron count rates is crucial for translating the observed lunar neutron count rate maps into water equivalent hydrogen (WEH) maps. Figure 3 demonstrates that we are able to correct every single observation of SETN and CSETN data by using LRO altitude information in addition to Oulu ground-based neutron observations needed for the Solar modulation correction.

Conclusions: Our studies show that the SETN's ^{3}He detector efficiency is the same as the efficiency of the CSETN's ^{3}He detectors. The ratio of SETN background noise to the total signal is relatively low, thus one can integrate all channels instead of using high channels only. This allows us to recover SETN observations after May 2011. We plan to translate the neutron flux maps into WEH maps by comparing the observations and the predicted count rates for each of the detectors.

References: [1] Mitrofanov, I. G., *et al.* (2009), *Astrobiology.*, 8(4) 793-804. [2] Mitrofanov *et a*l. (2010) *Sp. Sci. Rev.,* 150 (1-4). [3] Lawrence, D. J., *et al.*, (2010) Astrobiology 10(2). [4] Mitrofanov, I. G., *et al.* (2016), Instrum Exp Tech (2016) 59: 578. [5] T. P. McClanahan, *et al.*, (2018), *LPSC* #49 #TBD. [6] A. Parsons, *et al.*, (2018), *LPSC* #49 #TBD. [7] Usoskin, I. G. (2005), JGR J. Geophys. Res., 110, A12108. [8] Allison J. et al., (2006), *IEEE Trans. on Nucl. Sci.*, 53, 1. [9] McKinney, G.W., et al. (2006),. Geophys. Res., 111, E06004. [10] M.L. Litvak, *et al.*, (2016) *Plentary and Space Sci.*, 121 53-65.

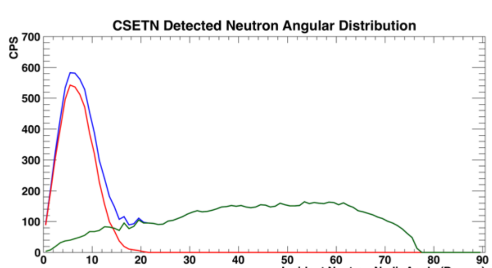

Figure 1. (Blue) The original energy distribution of the CSETN's total detected neutrons approaching the LEND/LRO at 50 km altitude. (Red) The energy distribution of detected neutrons before entering the CSETN ^{3}He detectors. (Green) Energy distribution of the detected neutrons with an incident angle greater than 15^{o}, *i.e.* uncollimated neutrons.

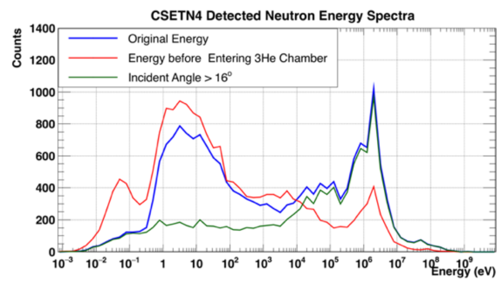

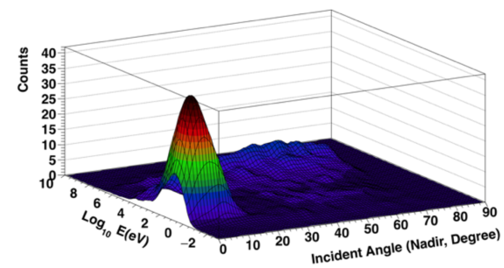

Figure 2. Top: (Blue) Total detected lunar neutrons, (Red) direct hit neutrons – without colliding with the collimators, other detectors or the LRO spacecraft body, (Green) detected scattered lunar neutrons. Bottom: Surface plot of the energy and incident angular distribution the CSETN's detected neutrons.

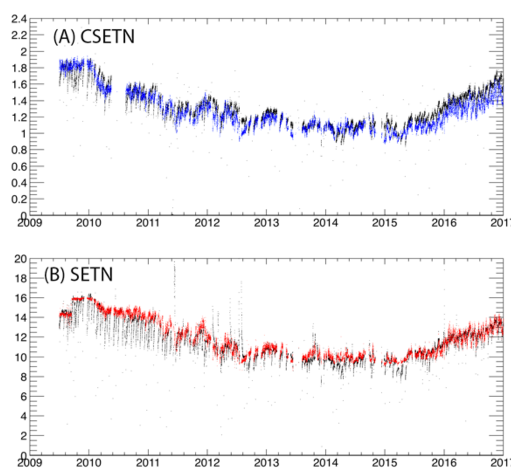

Figure 3. (A) Black – the observed CSETN high channel (Channel 7 to 15) total count rates, Blue – the predicted CSETN high channel count rates using Oulu neutron data and the LRO altitude. (B) Black – the observed SETN total count rates, Red – the predicted SETN total count rates.